ROTORFLOW: A quasi-simultaneous interaction method for the prediction of three-dimensional aerodynamic flow over wind turbine blades

H.A. Bijleveld, ECN

A.E.P.Veldman, University of Groningen

Paper presented at Torque 2010, June 28-30, Heraklion, Crete, Greece

November 2010

RotorFlow: A quasi-simultaneous interaction method for the prediction of three-dimensional aerodynamic flow over wind turbine blades

H.A. Bijleveld
ECN Wind Energy
P.O.Box 1, 1755 ZG Petten, the Netherlands
e-mail: bijleveld@ecn.nl

A.E.P. Veldman
Institute of Mathematics and Computing Science
University of Groningen
P.O.Box 407, 9700 AK Groningen, the Netherlands
e-mail: a.e.p.veldman@rug.nl

Abstract

For the numerical prediction of the aerodynamic forces on wind turbine blades, a viscous-inviscid interaction method is applied. From a discussion on the interaction methods, focussing on their ability to simulate separated flows, it follows that the quasi-simultaneous interaction method is the most suitable. The method employed here uses only the local influence of the external flow, resulting in an algebraic expression for the interaction-law equation. The method is applied to a model problem for a three-dimensional steady, incompressible, turbulent flow over a flat plate. For attached flow the quasi-simultaneous method converges to the same solution as a flow solver using a direct interaction method.

Keywords: viscous-inviscid interaction, boundary layer, three-dimensional flow, quasi-simultaneous interaction, wind turbine aerodynamics

1 Introduction

The increase in the size of wind turbines and their blades creates a need for more accurate prediction methods of the aerodynamic forces. Larger blades are more flexible, contain more material and therefore a higher level of accuracy in the applied design methods is desired. The goal of the RotorFlow project of ECN Wind Energy is to create a wind turbine rotor aerodynamics simulation code that requires little user expertise and computational effort, but can compute in detail the unsteady aerodynamic characteristics of rotor blades. The simulation of separated flows and the coupling of the code with structural dynamics programs will be feasible.

The rotor aerodynamics simulation code under development is a combination of a panel method flow solver for the three-dimensional, unsteady, incompressible, inviscid external flow (outer region) and an integral boundary-layer solver for the three-dimensional unsteady viscous flow near the blade surface (inner region), see Figure 1. The strong interaction between these two flow regions in separated flows will be accounted for by a so-called viscous-inviscid interaction method.

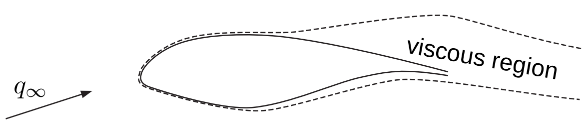

Figure 1: Domain decomposition into viscous and inviscid regions.

The interaction method ensures the exchange between the boundary-layer variables of the viscous flow and the inviscid flow variables. This method has extensively been applied in aerofoil applications (e.g. [11]), but is hardly used in the design of wind turbine blades.

This paper will focus on the application of a quasi-simultaneous interaction method for three-dimensional aerodynamic flow. First, background information about viscous-inviscid interaction methods is provided, followed by a description of the applied quasi-simultaneous method. To show that this method converges to the same solution as a direct method, the result of a simulation of a flow over a flat plate is discussed.

2 Viscous-Inviscid Interaction Methods

Since the development of the first viscous-inviscid interaction methods, several types of interaction methods have been developed. Four basic types of interaction methods will be discussed here from which other variants can be derived.

The philosophy of the interaction method is that it exchanges the velocity vector and the boundary-layer displacement thickness - modeled via a transpiration velocity - between the inviscid and viscous region until a smooth solution between the two regions is obtained.

Mathematically, the phenomenon of interaction can be described as follows:

$$\begin{cases} \vec{u}_e &= E\delta^* \\ \vec{u}_e &= B\delta^* \end{cases}, \qquad (1)$$

with $\vec{u}_e$ the velocity vector at the edge of the boundary layer; δ^* the boundary-layer displacement thickness; E and B the set of external flow and integral boundary-layer equations respectively.

The most straightforward method is the direct method. In this method, see Figure 2, the viscous and inviscid regions are calculated subsequently:

$$\begin{cases} \vec{u}_e^{(n)} &= E\delta^{*(n-1)} \\ \delta^{*(n)} &= B^{-1}\vec{u}_e^{(n)} \end{cases}, \qquad (2)$$

where n is the iteration number. This method works well for attached flows where the effect of the boundary layer on the external flow is small. However, at the point of separation a singularity occurs and B^{-1} cannot be determined. This is the well-known Goldstein singularity, already analyzed in 1948 [5].

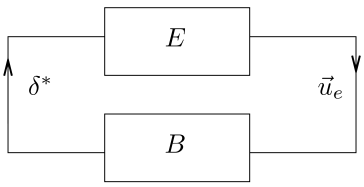

Figure 2: Direct interaction scheme.

Solving the boundary-layer equations with a given displacement thickness instead of a given velocity is referred to as an inverse method (Figure 3):

$$\begin{cases} \delta^{*(n)} &= E^{-1}\vec{u}_e^{(n-1)} \\ \vec{u}_e^{(n)} &= B\delta^{*(n)} \end{cases}. \qquad (3)$$

Catherall and Mangler [1] first proposed this method and this method is able to calculate separated flows. The convergence of the interaction scheme is slow, however.

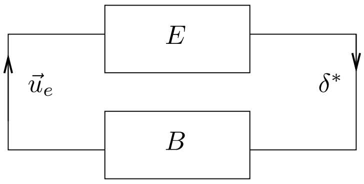

Figure 3: Inverse interaction scheme.

Both methods discussed before assume a hierarchy between the flow regimes. An alternative - to avoid the hierarchy - is to solve the viscous and inviscid flow simultaneously (Figure 4):

$$\begin{cases} \vec{u}_e^{(n)} - E\delta^{*(n)} &= 0 \\ \vec{u}_e^{(n)} - B\delta^{*(n)} &= 0 \end{cases}. \qquad (4)$$

This is a robust method and calculates separated flow well. The XFOIL code of Drela is based on this idea [3]. However, a drawback of this method is that the equations for both flows are modeled in one system of equations, reducing the flexibility in flow modeling and increasing software complexity.

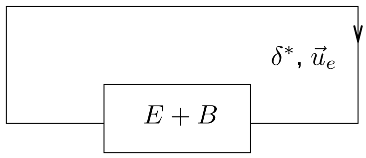

Figure 4: Simultaneous interaction scheme.

Using the advantages of the direct and simultaneous method and circumventing their drawbacks, is what the quasi-simultaneous method, developed by Veldman [12], is aiming for. This method solves the viscous flow region together with an *approximation* of the external flow and subsequently solves the inviscid flow, see Figure 5. The system of equations becomes:

$$\begin{cases} \vec{u}_e^{(n)} - I\delta^{*(n)} &= E\delta^{*(n-1)} - I\delta^{*(n-1)} \\ \vec{u}_e^{(n)} &= B\delta^{*(n)} \end{cases}$$
$$\Rightarrow (I - B)\delta^{*(n)} = (I - E)\delta^{*(n-1)}, \qquad (5)$$

where I is the approximation of the external flow which is called *interaction law*. The interaction law is formulated such that it has no influence on the converged solution: when $\delta^{*(n)} = \delta^{*(n-1)}$, I cancels from equation (5). In the past, several interaction laws have been applied, see for example Edwards [4] and Van der Wees and Van Muijden [11]. The interaction law applied in ROTORFLOW is based on the quasi-simultaneous interaction law formulation of Veldman.

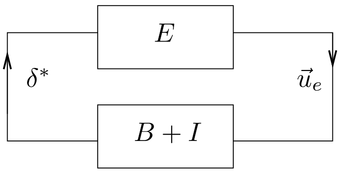

Figure 5: Quasi-simultaneous interaction scheme.

3 Interaction law

The interaction law I is a simplification of the external flow such that only the essentials of the inviscid flow are taken into account. The resulting interaction method closely resembles a direct method, with the advantage that separated flow can be calculated. The formulation of the interaction-law equation is based on thin-airfoil theory of which the three-dimensional derivation will be discussed in Section 4.

3.1 Interaction-law equation

For the formulation of the interaction-law equation, only the local influence of the external flow on the boundary layer is taken into account. This results in a very simple algebraic expression for the interaction law:

$$I:\ u_e + c q_\infty \delta^* = \mathrm{RHS}, \tag{6}$$

with c the interaction-law coefficient and q_∞ the absolute value of the upstream flow velocity. The right-hand side contains information of the external flow. For two-dimensional applications the interaction-law equation (6) is, [13]:

$$I_{2D}:\ u_e - \frac{4 q_\infty \delta^*}{\pi h} = \mathrm{RHS}, \tag{7}$$

where h is the mesh width from the discretization of the external flow model.

For three-dimensional applications we propose:

$$\begin{cases} I_{3D,u_e}:\ u_e - c_x q_e \delta_x = \mathrm{RHS}_x \\ I_{3D,v_e}:\ v_e - c_y q_e \delta_y = \mathrm{RHS}_y \end{cases} \tag{8}$$

Also, the q_∞ from (6) has been replaced by the local q_e, since combinations like $(q_e\delta_x)$ and $(q_e\delta_y)$ appear naturally in the formulation of the inviscid flow; see e.g. the source strength (20). The relation between the integral thicknesses δ_x, δ_y and the displacement thickness δ^* is given by Smith [10]. On an equidistant grid with $h = \Delta x = \Delta y$, the coefficients c_x and c_y become:

$$\begin{cases} c_x = -\frac{1}{h\pi}\ln\left|\frac{3+2\sqrt{2}}{3-2\sqrt{2}}\right| \\ c_y = -\frac{1}{h\pi}\ln\left|\frac{3+2\sqrt{2}}{3-2\sqrt{2}}\right| \end{cases}. \tag{9}$$

3.2 Comparison with direct method

For a two-dimensional boundary-layer flow it will be shown that for the direct method the set of integral boundary-layer equations B becomes singular at separation. It can also be shown that, for a suitably chosen constant c in equation (6), this singularity is removed by the additional interaction-law equation introduced in the quasi-simultaneous method. From Figure 6 it can be concluded that for the boundary-layer flow it is not possible to find a δ^* for every given u_e. The minimum in the u_e - δ^* curve corresponds with the point of separation at which also the H_1-H relation shows a minimum; the Goldstein singularity.

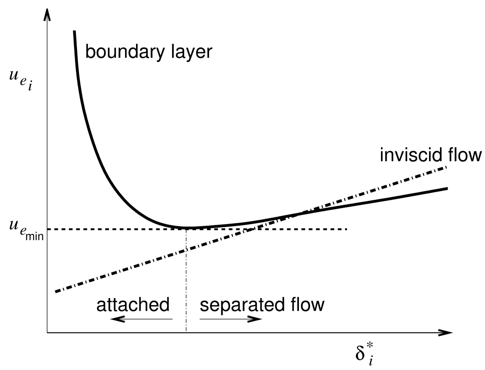

Figure 6: From [13]: Boundary layer and inviscid flow combined in terms of u_e and δ^*. Not for every slope of the inviscid flow relation a solution can be found.

For a two-dimensional flow, the boundary-layer can be described with the Von Kármán and Entrainment equations ([6], [9]). In the direct method, u_e is known and the system of equations can be written as: $\hat{F}\frac{\partial \mathbf{U}}{\partial x} = \mathrm{RHS_F}$, with $\mathbf{U} = (\delta^*, H)^T$ the vector of unknowns. The matrix $\hat{F}$ is:

$$\hat{F} = \begin{bmatrix} 1 & -\frac{\delta^*}{H} \\ \frac{H_1}{H} & \frac{\delta^*}{H}\left(\frac{\mathrm{d}H_1}{\mathrm{d}H} - \frac{H_1}{H}\right) \end{bmatrix} \tag{10}$$

and the right-hand side is:

$$\mathrm{RHS_F} = \begin{bmatrix} \frac{1}{2}c_f - \frac{\delta^*}{u_e}(2/H+1)\frac{\mathrm{d}u_e}{\mathrm{d}x} \\ C_E - \frac{H_1\delta^*}{u_e H}\frac{\mathrm{d}u_e}{\mathrm{d}x} \end{bmatrix}. \tag{11}$$

The right-hand side is assumed to be known. In the quasi-simultaneous interaction method, u_e is treated as an extra unknown with the interaction law as additional equation to close the system of equations. The interaction-law equation I_{2D} can be used to write u_e in terms of δ^* and subsequently be substituted into equation (10). The system of equations with the quasi-simultaneous interaction can be written as $\hat{F}^I \frac{\partial \mathbf{U}}{\partial x} = \mathrm{RHS}^\mathrm{I}$ with $\hat{F}^I$:

$$\hat{F}^I = \begin{bmatrix} 1 + C(2/H + 1) & -\frac{\delta^*}{H} \\ \frac{H_1}{H}(1 + C) & \frac{\delta^*}{H}\left(\frac{\mathrm{d}H_1}{\mathrm{d}H} - \frac{H_1}{H}\right) \end{bmatrix}, \quad (12)$$

where $C = -\frac{c\delta^*}{u_e} > 0$ and the right-hand side reduces to:

$$\mathrm{RHS}^I = \begin{bmatrix} \frac{1}{2}c_f \\ C_E \end{bmatrix}. \quad (13)$$

It is easily verified that the system of equations (10) becomes singular when $\frac{\mathrm{d}H_1}{\mathrm{d}H} = 0$ and the system (12) becomes singular when:

$$\frac{\mathrm{d}H_1}{\mathrm{d}H} = \frac{H_1}{H}\frac{C(1 + H)}{1 + C(2 + H)}. \quad (14)$$

The right-hand side of equation (14) is always positive for positive values of C. Figure 6 shows the relation between u_e and δ^* for inviscid flow as well. To obtain a robust interaction law the value of c should be chosen such that the slope of the interaction-law equation will always ensure an intersection with the viscous curve [13].

4 Model problem

A simulation of a boundary-layer flow over a flat plate is used to show that the quasi-simultaneous method (equation (5)) converges to the same result as the direct method (equation (2)). The boundary-layer flow is assumed to be steady, incompressible and turbulent. The external flow is a steady potential flow. For both flow regimes the models used by Coenen [2] are applied.

4.1 Boundary-layer flow

In the boundary-layer flow model three integral boundary-layer equations are employed together with suitable closure relations. The two integral momentum equations are in an orthogonal Cartesian coordinate system:

$$\frac{\partial}{\partial x}(\theta_{xx}q_e^2) + \frac{\partial}{\partial y}(\theta_{xy}q_e^2) = \\ - q_e\delta_x\frac{\partial u_e}{\partial x} - q_e\delta_y\frac{\partial u_e}{\partial y} + \tau_{w_x} \quad (15)$$

and

$$\frac{\partial}{\partial x}(\theta_{yx}q_e^2) + \frac{\partial}{\partial y}(\theta_{yy}q_e^2) = \\ - q_e\delta_x\frac{\partial v_e}{\partial x} - q_e\delta_y\frac{\partial v_e}{\partial y} + \tau_{w_y}. \quad (16)$$

The Entrainment equation reads:

$$\frac{\partial}{\partial x}(u_e\delta - q_e\delta_x) + \frac{\partial}{\partial y}(v_e\delta - q_e\delta_y) = q_eC_E, \quad (17)$$

with δ the boundary-layer thickness and θ_{xx}, θ_{xy}, θ_{yx} and θ_{yy} the x- and y-momentum thicknesses.

In the current model in the equation for θ_{sn}, equation (B.13) from [2], δ_s^* is replaced by δ_n^* according to the cited reference there.

The integral boundary-layer equations have to be extended with some closure relations, as in the two-dimensional case. In particular, following Houwink [8], the $H_1 - H$ relation is chosen such that it also can describe separated flow. In the final model for complete wind turbine blades, the closure relations can also contain effects of the rotating flow.

4.2 Inviscid flow

The external flow is assumed to be inviscid and irrotational. Therefore, it can be modeled by a potential flow in which the velocity potential can be described by equation (3.19) [2]:

$$\Phi = \phi + \Phi_\infty, \quad (18)$$

with

$$\phi = \frac{-1}{4\pi}\iint \frac{\sigma(x-\xi)\mathrm{d}\xi\mathrm{d}\eta}{((x-\xi)^2 + (y-\eta)^2 + Z_p^2)^{1/2}} \quad (19)$$

and the source strength σ is defined by equation (3.43) [2]:

$$\sigma = 2\left(\frac{\partial}{\partial x}(U_\infty Z_p) + \frac{\partial}{\partial y}(V_\infty Z_p)\right) \\ + 2\left(\frac{\partial}{\partial x}(q_e\delta_x) + \frac{\partial}{\partial y}(q_e\delta_y)\right). \quad (20)$$

This model applies only for flows over dented plates with Z_p the height of the plate. Furthermore, in equation (20) terms like $\frac{\partial q_e\delta_x}{\partial x}$ can be recognized which are related to the transpiration velocity.

4.3 Discretization of the external flow

For the calculation of the model problem, the geometry is divided into equally sized panels of size Δx by Δy on an orthogonal Cartesian grid. The velocity is obtained in the corner points of the panels. The derivatives of $(q_e\delta_x)$ and $(q_e\delta_y)$ from σ are discretized centrally. For the evaluation of the surface integral, expression (4.4.19) of Hess and Smith [7] is used. The external velocity at point (i, j) can be written as:

$$u_{e_{ij}} = \sum_{k=1}^{N_x+1} \sum_{l=1}^{N_y+1} [A^u_{ijkl} m_{x_{kl}} + B^u_{ijkl} m_{y_{kl}}] + u_{0_{e_{ij}}} \tag{21}$$

$$v_{e_{ij}} = \sum_{k=1}^{N_x+1} \sum_{l=1}^{N_y+1} [A^v_{ijkl} m_{x_{kl}} + B^v_{ijkl} m_{y_{kl}}] + v_{0_{e_{ij}}} \tag{22}$$

with $m_x = q_e \delta_x$, $m_y = q_e \delta_y$; $u_{0_{e_{ij}}}$, $v_{0_{e_{ij}}}$ follow from the terms in the first brackets of equation (20). The matrices A^u, B^u, A^v and B^v are called *influence matrices*.

For the coefficients c_x and c_y in the interaction-law equations (8), the local effect of the evaluation point is used: $(k, l) = (i, j)$. The elements of the influence matrices at that point are:

$$c_x = A^u_{ijij} = \frac{\Delta y}{2\pi \Delta x^2} \ln \left| \frac{(\sqrt{\Delta x^2 + \Delta y^2} + \Delta x)^2}{(\sqrt{\Delta x^2 + \Delta y^2} - \Delta x)^2} \right| ; \tag{23}$$

$$B^u_{ijij} = 0; \quad A^v_{ijij} = 0; \tag{24}$$

$$c_y = B^v_{ijij} = \frac{\Delta x}{2\pi \Delta y^2} \ln \left| \frac{(\sqrt{\Delta x^2 + \Delta y^2} + \Delta y)^2}{(\sqrt{\Delta x^2 + \Delta y^2} - \Delta y)^2} \right| . \tag{25}$$

The values of the influence matrices at $(k, l) = (i, j)$ are used as the interaction coefficients for the interaction law in the quasi-simultaneous interaction method applied (equation (8)).

4.4 Quasi-simultaneous implementation

The system of equations for the quasi-simultaneous interaction method, equation (5), is now fully modeled. Table 1 gives the corresponding equations.

Table 1: Equations implemented for the quasi-simultaneous interaction method, eq. (5).

E:	equations (21) and (22)
B:	equations (15), (16) and (17)
I:	equation (8)

The three integral boundary-layer equations B and the interaction-law equations I are written in one system of equations: $(B + I)\mathbf{U} = 0$. The vector of unknowns $\mathbf{U}$ contains:

$$\mathbf{U} = (u_e, v_e, H, \theta_{ss}, \beta)^T. \tag{26}$$

The boundary-layer equations are discretized with a finite difference upwind scheme. The resulting system of equations is solved via Newton iteration. The following initial solution is used:

$$\begin{aligned} u_e &= 1.0; \\ v_e &= 0.0; \\ H &= 1.35; \\ \theta_{ss} &= 0.005/(Re^{0.2}); \\ \beta &= 0.0, \end{aligned}$$

where $Re = 11.5 \times 10^6$ and β is the angle between the external streamline and the limiting wall streamline.

5 Results

The quasi-simultaneous interaction method has been implemented to perform a simulation of flow over a flat plate with an equidistant grid both in x- and y-directions with $N_x = N_y = 17$; $\Delta x = \Delta y = 1/16$.

The total calculation time strongly depends on the determination of the values of the influence matrices whose size scales with $(N_x \times N_y)^2$. The influence matrices are determined before the interaction cycle - Figure 5 - starts. For converged solutions less than ten sweeps through the interaction cycle are needed.

The applied external flow is two-dimensional and the boundary-layer is assumed to show two-dimensional behavior as well. In Figure 7 and 8 the shape factor and displacement thickness of a 2D and 3D simulation are shown. From the figure it follows that the results match well.

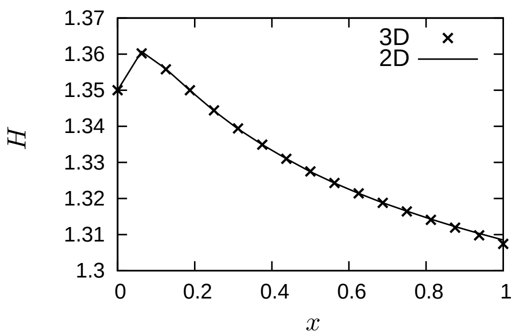

Figure 7: Comparison between a 2D and the 3D model - shape factor, $\Delta x = \frac{1}{16}$, $Re = 11.5 \times 10^6$.

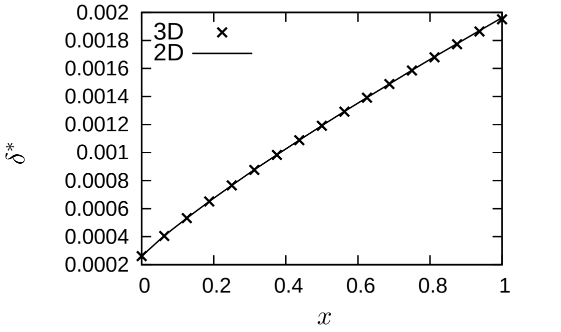

Figure 8: Comparison between a 2D and the 3D model - displacement thickness, $\Delta x = \frac{1}{16}$, $Re = 11.5 \times 10^6$.

For simulations with several mesh sizes on the three-dimensional grid, Table 2 shows the values of the streamwise velocity, δ_x and shape factor. The table shows that the differences for the resulting values of the boundary-layer variables are very small.

Table 2: Boundary-layer variables for several grid sizes at $x = 1.0$, $y = 0.5$ for flow over a flat plate with $Re = 11.5 \times 10^6$, $h = \Delta x = \Delta y$.

h	u_e	δ_x	H
$1/8$	1.002	1.939×10^{-3}	1.307
$1/16$	1.002	1.950×10^{-3}	1.307
$1/32$	1.002	1.956×10^{-3}	1.307
$1/64$	1.002	1.956×10^{-3}	1.307

The interaction law of the quasi-simultaneous method is applied in defect formulation and has no influence on the converged solution, see also equation (5). Figures 9 and 10 show the shape factor and streamwise momentum thickness for calculations with the quasi-simultaneous and direct method, respectively. It can be seen that the results for both methods coincide. The differences between the results are of $\mathcal{O}\left(10^{-4}\right)$. Figure 11 shows the vector plot of the two simulations. In this figure it can also be observed that both methods converge to the same solution as the vectors coincide.

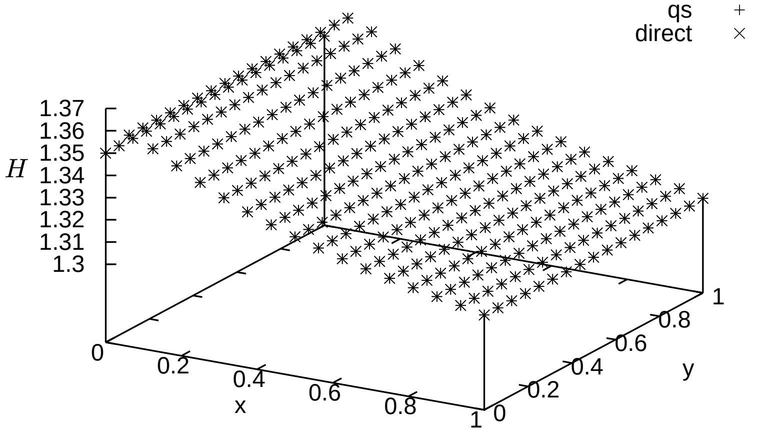

Figure 9: Shape factor of a simulation with the direct and quasi-simultaneous method, $\Delta x = \Delta y = \frac{1}{16}$, $Re = 11.5 \times 10^6$.

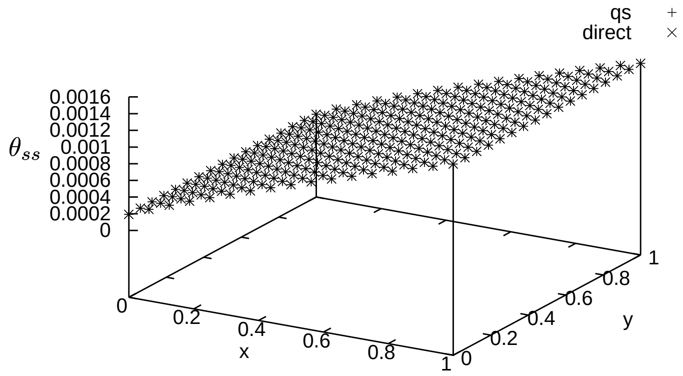

Figure 10: Streamwise momentum thickness of a simulation with the direct and quasi-simultaneous method, $\Delta x = \Delta y = \frac{1}{16}$, $Re = 11.5 \times 10^6$.

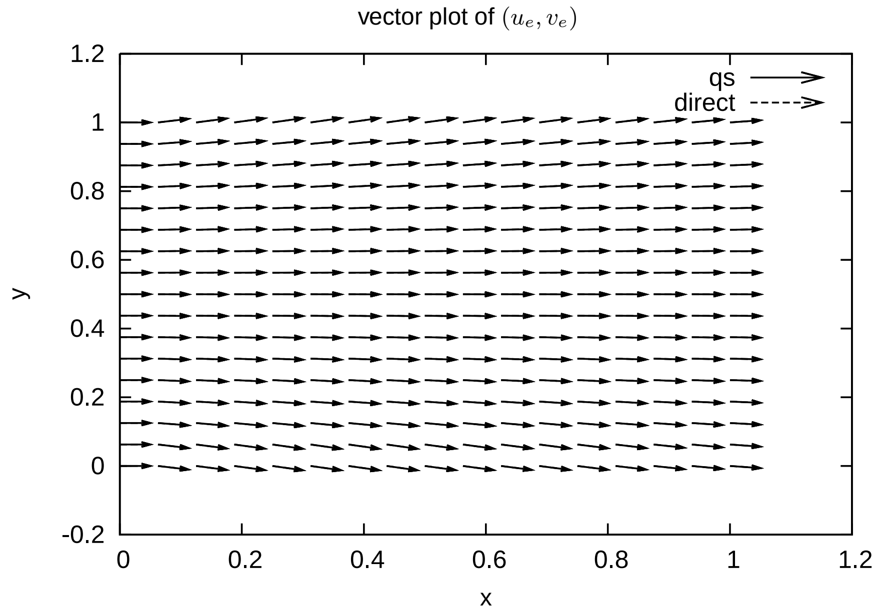

Figure 11: Vector plot of velocity of a simulation with the direct and quasi-simultaneous method, $\Delta x = \Delta y = \frac{1}{16}$, $Re = 11.5 \times 10^6$. Note that the vectors of both simulations coincide at every point calculated.

6 Conclusion

For the interaction between the inviscid and viscous flow regimes in RotorFlow, a three-dimensional formulation for the quasi-simultaneous interaction method has been derived. The applied interaction-law equation is based on the local influence of the inviscid flow on the boundary-layer. The method has been applied on a steady, incompressible, turbulent flow over a flat plate. It was shown that for a two-dimensional flow over a three-dimensional flat plate, the result matches with a fully two-dimensional calculation. The mesh size hardly influences the final result for the problem considered. Furthermore, the result also coincides with a result of a simulation using a direct method.

Future tests for the quasi-simultaneous interaction law as derived here include the simulation of a boundary-layer flow over a dented plate including separation and substitution of the algebraic interaction-law equation into the partial differential equations of the integral boundary-layer equations making the set of equations suitable for application in other flow solvers.

Acknowledgements The authors would like to thank the other members of the ECN Wind Energy ROTORFLOW project team for the support and fruitful discussions. The financial support by the ministry of Economical Affairs of The Netherlands is gratefully acknowledged. This research is carried out under contract of the InnWind project of SenterNovem (Agentschap NL).

References

[1] D. Catherall and K.W. Mangler. The integration of the two-dimensional laminar boundary-layer equations past the point of vanishing skin friction. *Journal of Fluid Mechanics*, 26:163–182, 1966.

[2] E.G.M. Coenen. *Viscous-Inviscid Interaction with the Quasi-Simultaneous Method for 2D and 3D Aerodynamic Flow*. PhD thesis, Rijksuniversiteit Groningen, the Netherlands, 2001.

[3] M. Drela. XFOIL: An analysis and design system for low Reynolds number airfoils. *Low Reynolds Numbers Aerodynamics*, 1989.

[4] D.E. Edwards. Analysis of three-dimensional flow using interacting boundary-layer theory. In F.T. Smith and S.N. Brown, editors, *Proc. IUTAM Symposium on boundary-Layer separation*, pages 163–178, 1987.

[5] S. Goldstein. On laminar boundary layer flow near a point of separation. *Quart J Mech Appl Math*, 1:43–69, 1948.

[6] M.R. Head. Entrainment in the turbulent boundary layer. Technical report, Aeronautical Research Council R&M 3152, 1960.

[7] J.L. Hess and A.M.O. Smith. Calculation of potential flow about arbitrary bodies. *Progress in Aerospace Sciences*, 8:1–138, 1967.

[8] R. Houwink and A.E.P. Veldman. Steady and unsteady flow computations for transonic airfoils. *AIAA*, 84-1618, 1984.

[9] H. Schlichting and K. Gersten. *Boundary Layer Theory, 8th Revised and Enlarged Edition*. Springer-Verlag, 1999.

[10] P.D. Smith. An integral prediction method for three-dimensional compressible turbulent boundary layers. Technical Report R&M 3739, Aeronautical Research Council, 1974.

[11] A.J. van der Wees and J. van Muijden. A robust quasi-simultaneous interaction method for a full potential flow with a boundary layer with application to wing/body configurations. In *Proceedings of the 5th symposium on numerical and physical aspects of aerodynamic flows*, 1992.

[12] A.E.P. Veldman. New, quasi-simultaneous method to calculate interacting boundary layers. *AIAA Journal*, 19:79–85, 1981.

[13] A.E.P. Veldman. A simple interaction law for viscous-inviscid interaction. *Journal of Engineering Mathematics*, 65:367–383, 2009.

Table 3: List of symbols

A^u, A^v, B^u, B^v	Influence matrices
B, E, I	System of boundary-layer, external flow and interaction law equations respectively
c, c_x, c_y, C	Interaction-law coefficients
C_E	Entrainment coefficient
c_f	Skin-friction coefficient
$\hat{F}$	System of 2D boundary-layer equations
H	Shape factor
H_1	$\frac{\delta-\delta^*}{\theta}$
h, Δx, Δy	Mesh width
N_x, N_y	Number of mesh points
n	Iteration number
q_∞, q_e	Absolute value of flow velocity upstream and at the edge of the boundary layer
Re	Reynolds number
RHS	Right-hand side of an equation
$\vec{u} = \{u_{e_{ij}}, v_{e_{ij}}\}^T$	Boundary-layer edge velocity vector
$\mathbf{U}$	Vector of unknowns
β	Angle between external streamline and limiting wall streamline
δ	Boundary-layer thickness
δ^*	Boundary-layer displacement thickness
δ_x, δ_y	Boundary-layer integral thicknesses
θ_{xx}, θ_{xy}, θ_{yx}, θ_{yy}	Boundary-layer momentum thicknesses in x, y-coordinates
θ_{ss}	Boundary-layer momentum thickness in streamwise direction
Φ, ϕ, σ	Flow potential and source strength for external flow modeling
τ_{wx}, τ_{wy}	Skin-friction